

Influence of laser intensity on absorption line broadening in laser absorption spectroscopy

Makoto Matsui^{a),b)} and Kimiya Komurasaki^{a)}

Department of Advanced Energy, The University of Tokyo, 5-1-5 Kashiwanoha, Kashiwa, 277-8583 Chiba, Japan

Satoshi Ogawa^{c)} and Yoshihiro Arakawa^{c)}

Department of Aeronautics and Astronautics, The University of Tokyo, 7-3-1 Hongo, Bunkyo, 113-8656 Tokyo, Japan

(Received 2 August 2005; accepted 27 July 2006; published online 22 September 2006)

The influence of laser intensity on absorption line broadening was investigated. Laser absorption spectroscopy was applied to low-pressure plasma, and the translational temperature deduced from the Doppler width was found to increase with laser intensity; this was in contrast to the conventional laser theory. Consequently, the dependency of absorption saturation on the Doppler frequency was considered. The predicted variation in broadening width with laser intensity showed a good agreement with the measurement. In addition, we obtained a correction factor for the temperature measurement at high laser intensity. © 2006 American Institute of Physics.

[DOI: 10.1063/1.2353893]

I. INTRODUCTION

Laser absorption spectroscopy is a useful diagnostic technique that is applicable even to optically thick plasma. The translational temperature and the number density of the absorbing particles are obtained by analyzing an absorption line shape.¹⁻³ The absorption lines generally exhibit a Voigt profile, which is a convolution of homogeneous (Lorentzian) and inhomogeneous (Gaussian) broadenings. In Doppler broadening, the square of its width is proportional to the translational temperature; it is an inhomogeneous broadening and is distinguishable from the others by Voigt fitting. This is because all the other broadenings such as Stark, natural, pressure (collision), and saturation broadenings are homogeneous.

In contrast to the conventional laser theory, the Doppler broadening in low-pressure plasma has been experimentally found to be strongly influenced by the probe laser intensity.^{4,5} Although similar inconsistencies in measured Doppler broadening simulation have been reported in neon and argon plasmas at a pressure of less than 100 Pa,^{6,7} a clear explanation has not been obtained thus far. This study specifically addresses the relationship between Doppler broadening and laser intensity.

II. THEORY

According to the conventional theory, a saturated absorption line shape $k_S(\nu)$ is a convolution integral of the Gaussian and the Lorentzian profiles and is expressed as

$$k_S(\nu) = K_0 \frac{2\sqrt{\ln 2} \Delta\nu_L}{\pi^{3/2} \Delta\nu_D} \times \int_{-\infty}^{\infty} \frac{\exp\{-[2(\nu_\xi - \nu_0)/\Delta\nu_D]^2 \ln 2\} d\nu_\xi}{(\nu - \nu_\xi)^2 + (\Delta\nu_L \sqrt{1 + III_{S_inhomo}})^2/4}. \quad (1)$$

Here, ν , ν_0 , and ν_ξ represent laser frequency, absorption line frequency, and integral variable, respectively. K_0 , $\Delta\nu_L$, and $\Delta\nu_D$ are the unsaturated integrated absorption coefficient, Lorentzian width, and Doppler width, respectively. The Doppler width is related to the deduced temperature T as follows:

$$T = \left(\frac{\Delta\nu_D}{2\sqrt{2 \ln 2}} \right)^2 \frac{mc^2}{k_B \nu_0^2}. \quad (2)$$

Here, m , c , and k_B are the mass of the absorbers, velocity of light, and the Boltzmann constant, respectively. The saturation laser intensity of inhomogeneous broadening I_{S_inhomo} is defined as

$$I_{S_inhomo} = \frac{2\pi^2 h \nu^3 \Delta\nu_L}{\phi c^2}. \quad (3)$$

Here, h is Planck's constant and $\phi = A_{ji}/(A_{ji} + Q_{ji})$, where A , Q , i , and j represent the Einstein coefficient, quenching rate, absorption level, and excited level, respectively. When the pressure broadening predominated in homogeneous broadening, Eq. (3) is rewritten as

$$I_{S_inhomo} = \frac{2\pi^2 h \nu^3 N \bar{v} \sigma}{\phi c^2}. \quad (4)$$

Here, N and σ represent the number density of the colliding particles and collision cross section, respectively.⁸ \bar{v} is the average velocity of the absorbers, which is defined as $\bar{v} = \sqrt{3k_B T/m}$.

^{a)}FAX: +81-4-7136-4030.

^{b)}Electronic mail: matsui@al.t.u-tokyo.ac.jp

^{c)}FAX: +81-3-5841-6586.

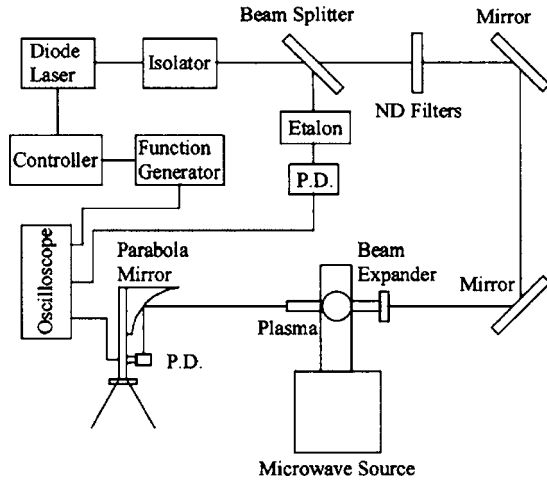


FIG. 1. Measurement system.

Equation (1) shows that the Doppler width of the saturated profile is unaffected by the variation in laser intensity, whereas its Lorentzian width $\Delta\nu_{SL}$ increases with laser intensity,

$$\Delta\nu_{SL} = \Delta\nu_L \sqrt{1 + III_{S_inhomo}} \tag{5}$$

Equation (1) also shows that $k_S(\nu)$ continues to exhibit Voigt profile, and the relationship between the saturated integrated absorption coefficient K_S and K_0 can be expressed by the following equation:³

$$K_S = \int k_S(\nu) d\nu = \frac{K_0}{\sqrt{1 + III_{S_inhomo}}} \tag{6}$$

III. EXPERIMENT

A. Experimental setup

A schematic of the measurement system is shown in Fig. 1. The influence of laser intensity on the broadenings was measured in two types of argon plasma: a glow discharge plasma with an input power, discharge voltage, and ambient pressure of 1.5 W, 300 V, and 79 Pa, respectively, and a

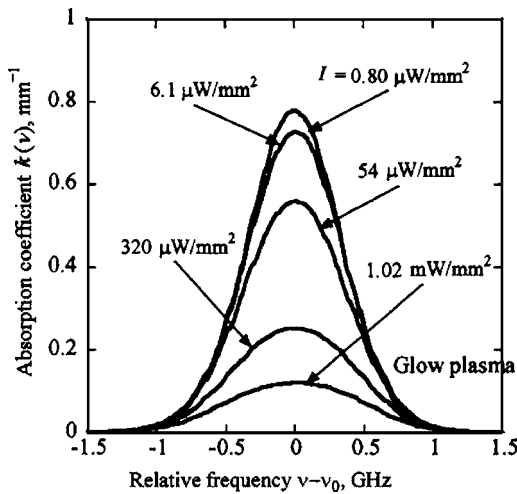


FIG. 2. Variation in the absorption profiles of the glow discharge argon plasma. $\nu_0=842.46$ nm.

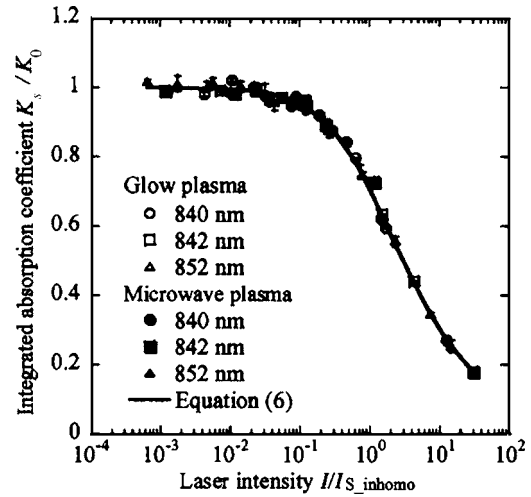


FIG. 3. Relationship between absorption coefficient and laser intensity.

TE₁₀ mode microwave discharge plasma with an input power, oscillation frequency, mass flow rate, and ambient pressure of 500 W, 2.4 GHz, 20 SCCM (SCCM denotes cubic centimeter per minute at STP), and 20 Pa, respectively. A tunable diode laser (DMD845; Environmental Optical Sensors, Inc.) with an external cavity and a linewidth of less than 300 kHz was used as a probe. The probe laser intensity was measured using a photodetector (DET110; Thorlab, Inc.). The intensity was changed from 0.60 $\mu\text{W}/\text{mm}^2$ to 5.44 mW/mm^2 by using a combination of neutral density filters and a beam expander. An etalon was used as a wavemeter. Its free spectral range was 0.75 GHz and the frequency was calibrated by linear interpolation. The target absorption lines of ArI were 840.82, 842.46, and 852.14 nm.⁹

B. Experimental results

Figure 2 shows the measured absorption profiles at the 842.46 nm line in the glow discharge plasma. Strong absorption saturation was observed at high laser intensity. Absorption saturation was also observed for the other lines and in the microwave discharge plasma. With regard to the

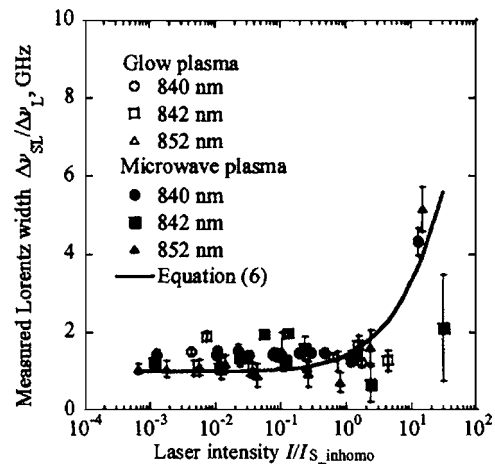


FIG. 4. Measured Lorentzian width.

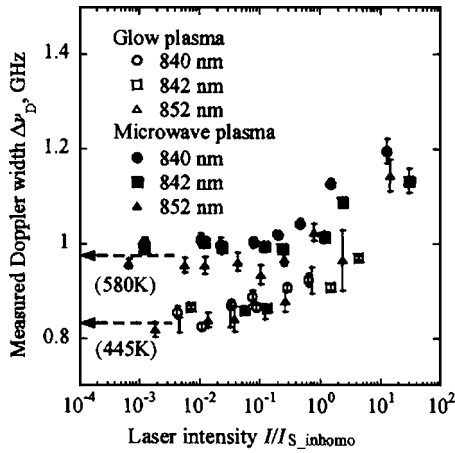


FIG. 5. Measured Doppler width.

measured profiles, K_S , $\Delta\nu_{SL}$, and $\Delta\nu_D$ were obtained by Voigt fitting. Here, a nonlinear fitting software (ORIGIN PRO 6.1; Origin Lab, Inc.) was used.

Figure 3 shows a plot of the measured K_S/K_0 and a theoretical curve fitting of Eq. (6) as a function of III_{S_inhomo} , where K_0 and I_{S_inhomo} are fitting parameters. K_S/K_0 was very close to the theoretical curve and K_0 was deduced within a 5% error at an III_{S_inhomo} of less than 0.1. Figure 4 shows a plot of the measured $\Delta\nu_{SL}/\Delta\nu_L$ and a theoretical curve fitting of Eq. (5) as a function of III_{S_inhomo} , where $\Delta\nu_L$ is a fitting parameter. $\Delta\nu_{SL}/\Delta\nu_L$ was almost close to the theoretical curve. At an III_{S_inhomo} of greater than 10, $\Delta\nu_{SL}/\Delta\nu_L$ was smaller than that predicted in Eq. (5). Figure 5 shows a plot of the measured $\Delta\nu_D$ as a function of III_{S_inhomo} . In contrast to the theoretical prediction of Eq. (1), $\Delta\nu_D$ increased with I , thereby resulting in an increase in T with I . The temperatures of the glow and microwave plasmas at III_{S_inhomo} of 0 were estimated to be 445 and 580 K, respectively.

IV. DISCUSSION

A. Dependency of I_{S_inhomo} on the frequency

One reason of the above contradiction might be that the temperature actually increased with I by laser heating. However, most of the absorbed energy is transferred not to the

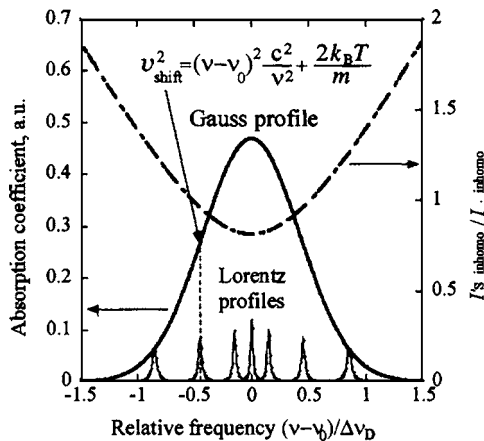


FIG. 6. Conceptual absorption profile and $I'_{S_inhomo}/I_{S_inhomo}$.

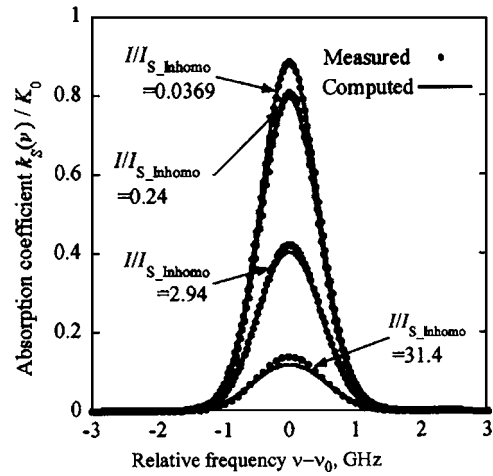


FIG. 7. Measured and computed profiles of the 842.46 nm line.

translational energy but to the emission one because transition rate of the spontaneous emission is one order of magnitude greater than that of the inelastic collision with electrons and four orders than that with atoms.¹⁰

Then, we consider the dependency of I_{S_inhomo} on the relative frequency $|\nu - \nu_0|$. The averaged velocity seen in Eq. (4) may be a function of $|\nu - \nu_0|$. In fact, the absorbers that exhibit a larger Doppler shift in a Gaussian distribution have a higher velocity component in the laser beam direction. On the other hand, the velocity component in the other two directions has a thermal velocity of $k_B T_0/m$, respectively, because of its independency on $|\nu - \nu_0|$. Subsequently, in an isotropic gas in a three-dimensional velocity field, the average velocity $v_{shift}(\nu)$ of the absorbers exhibiting the Doppler shift $|\nu - \nu_0|$ is expressed as

$$v_{shift}(\nu) = \sqrt{(\nu - \nu_0)^2 \frac{c^2}{\nu_0^2} + \frac{2k_B T_0}{m}}$$

$$= \bar{v} \sqrt{\frac{8 \ln 2}{3} \frac{(\nu - \nu_0)^2}{\Delta\nu_D^2} + \frac{2}{3}} \tag{7}$$

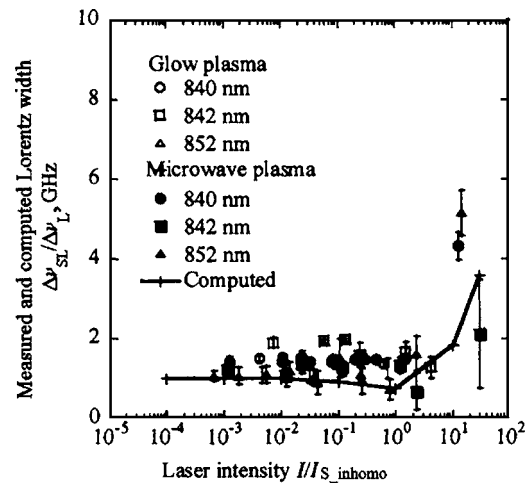


FIG. 8. Measured and computed Lorentzian width.

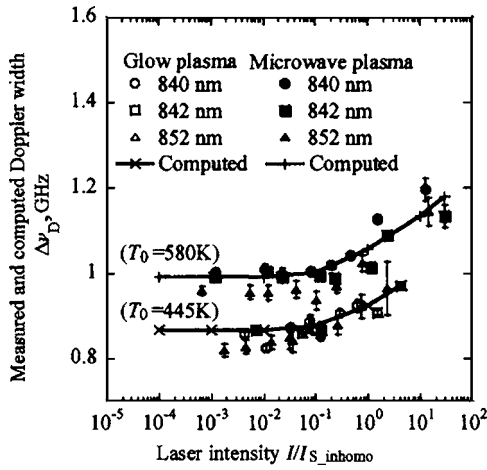


FIG. 9. Measured and computed Doppler width.

Here, T_0 is the true temperature and $\bar{v} = \sqrt{3k_B T_0/m}$. Under the assumption that σ is constant, the saturation laser intensity with respect to the velocity distribution I'_{S_inhomo} is redefined by substituting Eq. (7) into Eq. (4) as

$$g(\nu) = \frac{2\sqrt{\ln 2} \Delta\nu_L}{\pi^{3/2} \Delta\nu_D} \int_{-\infty}^{\infty} \frac{\exp[-2(\nu_\xi - \nu_D)/\Delta\nu_D]^2 \ln 2 d\nu_\xi}{(\nu - \nu_\xi)^2 + \{\Delta\nu_L \sqrt{1 + III_{S_inhomo} \sqrt{(8 \ln 2/3)[(\nu - \nu_0)^2/\Delta\nu_D^2 + (2/3)]}}\}^2/4}. \quad (9)$$

In Fig. 7, the computed absorption profiles of the 842.46 nm line for various III_{S_inhomo} with $\Delta\nu_L$ and $\Delta\nu_D$ measured at the lowest III_{S_inhomo} (MATHEMATICA 4.0; Wolfram Research, Inc.) are compared to the measured profiles. Both profiles were found to be similar.

Figures 8 and 9 show the plots of the measured and computed $\Delta\nu_{SL}/\Delta\nu_L$ and $\Delta\nu_D$, respectively, as a function of III_{S_inhomo} . Here, the computed $\Delta\nu_{SL}/\Delta\nu_L$ and $\Delta\nu_D$ were obtained by Voigt fitting. The results of both experiments showed a good agreement with the computation.

The ratio of deduced temperature to true temperature was computed for various laser intensities and Voigt parameters $\alpha = \sqrt{\ln 2} \Delta\nu_L/\Delta\nu_D$ of the measured profiles, as tabulated in Table I. When the probe laser intensity is high ($III_{S_inhomo} > 10^{-1}$), the temperature will be overestimated and should be corrected by the factor given in Table I.

V. CONCLUSION

When the probe laser intensity I is high, the Doppler broadening of the absorption line becomes wider, and the temperature deduced from the broadening tends to be overestimated. This is caused by the dependency of the saturation intensity I_{S_inhomo} on the frequency. The absorbers that exhibit

TABLE I. Ratio of deduced temperature to true temperature (T/T_0).

α	III_{S_inhomo}					
	10^{-4}	10^{-3}	10^{-2}	10^{-1}	1	10
0.01	1.000	1.000	1.002	1.021	1.109	1.229
0.05	1.000	1.000	1.003	1.024	1.145	1.347
0.1	1.000	1.000	1.003	1.027	1.172	1.516

$$I'_{S_inhomo} = I_{S_inhomo} \sqrt{\frac{8 \ln 2 (\nu - \nu_0)^2}{3 \Delta\nu_D^2} + \frac{2}{3}}. \quad (8)$$

Figure 6 shows a conceptual absorption profile and the theoretical plot of $I'_{S_inhomo}/I_{S_inhomo}$. At $\nu = \nu_0 \pm \Delta\nu_D$, I'_{S_inhomo} is almost twice as large as that of $\nu = \nu_0$.

B. True temperature

Substituting Eq. (8) into Eq. (1), the line shape function $g(\nu) = k_S(\nu)/K_0$ of the absorption profile is expressed as

a larger Doppler shift $|\nu - \nu_0|$ have a higher average velocity; as a result, I_{S_inhomo} increases with an increase in the relative frequency $|\nu - \nu_0|$.

Although the probe laser intensity is high and the saturation effect is large, the true temperature can be obtained by using the correction factor presented in this study.

ACKNOWLEDGMENTS

This research was partially supported by the Ministry of Education, Science, Sports and Culture, Grant-in-Aid for Scientific Research (B), 14350507, 2002 and Research Fellowships of the Japan Society for the Promotion of Science for Young Scientists 16-10857.

¹M. Matsui, Y. Oda, H. Takayanagi, K. Komurasaki, and Y. Arakawa, *Vacuum* **73**, 341 (2004).

²F. Y. Zhang, T. Fujiwara, and K. Komurasaki, *Appl. Opt.* **40**, 957 (2001).

³D. S. Bear and R. K. Hanson, *Appl. Opt.* **32**, 948 (1993).

⁴C. Davis, *Lasers and Electronics* (Cambridge University Press, Cambridge, 1996).

⁵A. Yariv, *Quantum Electronics*, 2nd ed. (Wiley, New York, 1989).

⁶A. C. Linday, J. L. Nicol, and D. N. Stacey, *J. Phys. B* **24**, 4901 (1991).

⁷S. Kasai, R. Mizutani, R. Kondo, M. Hasuo, and T. Fujimoto, *J. Phys. Soc. Jpn.* **72**, 1936 (2003).

⁸W. Demtroder, *Laser Spectroscopy*, 2nd ed. (Springer, Berlin, 1996).

⁹NIST Atomic Spectra Database, http://physics.nist.gov/cgi-bin/AtData/main_asd

¹⁰J. Vlcek, *J. Phys. D* **22**, 623 (1989).